

# Dynamic cancellation of ac Stark shift for pulsed EIT/Raman optical lattice clocks

Thomas Zanon-Willette, Andrew D. Ludlow, Sebastian Blatt, Martin M. Boyd, Ennio Arimondo,\* Jun Ye  
*JILA, National Institute of Standards and Technology and University of Colorado,  
 Department of Physics, University of Colorado, Boulder, Colorado 80309-0440, USA*  
 (Dated: March 31, 2022)

We propose a combination of Electromagnetically Induced Transparency (EIT)/Raman and pulsed spectroscopy techniques to accurately cancel frequency shifts arising from EIT fields in forbidden optical lattice clock transitions of alkaline earth atoms. Time-separated laser pulses are designed to trap atoms in coherent superpositions while eliminating off-resonance ac Stark contributions at particular laser detunings from the intermediate excited state. The scheme achieves efficient population transfer up to 60% with potential inaccuracy  $< 10^{-17}$ . Both complex wave-function formalism and density matrix approach predict cancellation of external light shifts at the mHz level of accuracy, under low field strengths or short interaction times.

PACS numbers: 32.80.-t, 42.62.Eh, 42.50.Gy, 32.70.Jz

In the field of optical frequency standards and clocks, single trapped ions [1] and alkaline earth atoms [2, 3, 4, 5, 6] are advancing clock performances. The advantage arises from superhigh resonance quality factors of these optical transitions [7], which are expected to be  $10^5$  better than microwave fountains. These fountain clocks are already below the  $10^{-15}$  relative fractional uncertainty [8]. Fermionic isotopes of alkaline earths trapped in optical lattices at the magic wavelength [9] offer ultra narrow linewidths of a few mHz without recoil and Doppler effects, but remain potentially sensitive to systematic effects arising from the nuclear spin-related tensor polarizability [3, 4, 5]. On the other hand, bosonic isotopes with no nuclear spin and a higher natural isotopic abundance avoid multiple hyperfine components but lack direct excitation of the clock transition  $|1\rangle \leftrightarrow |2\rangle$  in Fig. 1(a). Indirect excitation via continuous-wave Electromagnetically Induced Transparency (EIT) has been proposed to probe these forbidden transitions [10, 11]. A similar scheme for the  $^{174}\text{Yb}$  forbidden clock transition was implemented by applying a dc magnetic field for state mixing [6].

All such schemes can suffer from Stark shifts due to non-resonant electric-dipole couplings of the clock levels to other states induced by the applied electromagnetic fields [12, 13]. Ref. [10] provides some detailed calculations of these shifts. To further reduce this potential systematic error, we could apply an approach similar to that used for the determination of the magic wavelength [3, 4] or the hyperpolarizability contribution to the ac Stark shifts [14]: Measurements at different field strengths are used to extrapolate the clock frequency to vanishing field. However, this simple approach does not apply to the EIT-related schemes where the applied field strength modifies also the optical pumping time required to prepare the atoms in a coherent superposition [15]. The preparation time required for optimal signal contrast and clock stability becomes unpractically long at low field strengths. But using large fields increases the ac Stark shifts and limits the clock accuracy. To overcome these limits, the pulsed scheme proposed in this Letter (Fig. 1(c)) optimizes clock performance by utilizing time-separated laser

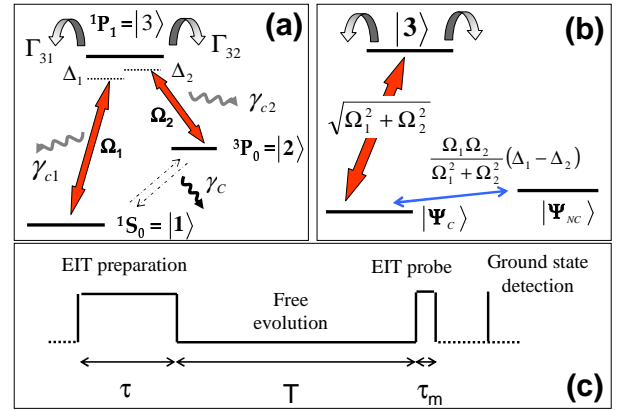


FIG. 1: (Color online)(a) Three level atom-light configuration for an optical lattice clock based on time-separated laser pulses including relaxation and decoherence rates. The optical detunings  $\Delta_1 \equiv \Delta_0 + \eta_1$ ,  $\Delta_2 \equiv \Delta_0 - \delta_r + \eta_2$  include ac Stark-shifts  $\eta_i$  from off-resonant levels. Here  $\Delta_0$  is the common mode detuning and  $\delta_r$  denotes deviation from the Raman condition. (b) The corresponding dressed-state representation of bright  $|\Psi_C\rangle$  and dark  $|\Psi_{NC}\rangle$  states defining the clock transition. (c) The probing pulse sequence.

pulses to prepare and interrogate the optical clock transition [16]. It is an original mix of Ramsey spectroscopy [17] and highly efficient population transfer under Coherent Population Trapping (CPT) [18]. The first pulse prepares atoms in a coherent superposition and the second pulse probes the clock frequency. This configuration produces a large contrast in the detected clock signal. More importantly, as the detunings of the applied fields affect the phase evolution of the atomic wave-function, a proper combination of the common mode laser detuning  $\Delta_0$  and pulse durations  $\tau, \tau_m$  (Fig. 1) reduces the clock shift to  $\sim 10^{-17}$ . The discussion presented here reveals for the first time a general relation connecting the preparation time of the Raman coherence and the signal contrast in the subsequent detection of this coherence, relevant to many EIT or CPT related experiments.

The atomic evolution between  $^1S_0$  and  $^3P_0$  is properly

described in the dressed state picture (Fig. 1(b)),

$$\begin{aligned} |1\rangle &= \frac{\Omega_1}{\sqrt{\Omega_2^2 + \Omega_1^2}} |\Psi_C\rangle + \frac{\Omega_2}{\sqrt{\Omega_2^2 + \Omega_1^2}} |\Psi_{NC}\rangle \\ |2\rangle &= \frac{\Omega_2}{\sqrt{\Omega_2^2 + \Omega_1^2}} |\Psi_C\rangle - \frac{\Omega_1}{\sqrt{\Omega_2^2 + \Omega_1^2}} |\Psi_{NC}\rangle \end{aligned} \quad (1)$$

where  $\Omega_1$  and  $\Omega_2$  are the Rabi frequencies for the transitions  $^1S_0 \leftrightarrow ^1P_1$  and  $^3P_0 \leftrightarrow ^1P_1$ . For an ideal 3-level system described in Eq. (1), the dark state  $|\Psi_{NC}\rangle$  remains insensitive to light shift, while the bright state  $|\Psi_C\rangle$  is always coupled to the laser light. A realistic atomic clock has to deal with off-resonant ac Stark shifts acting on  $|\Psi_C\rangle$  while atoms are pumped into  $|\Psi_{NC}\rangle$  with a few spontaneous emission cycles. Thus, a judicious trade-off between the short-time dynamics for a high-contrast signal (large optical pumping) and the reduced external ac shifts (and resonance power broadenings) under a low field strength needs to be found for practical realizations of these EIT/Raman-type clocks.

To describe our pulsed method, we start from a three-level configuration as shown in Fig. 1(a). The Optical Bloch Equations (OBEs) describe three-level dynamics including external shifts, relaxations, and decoherences between atomic states [19] in terms of the density matrix:

$$\dot{\rho} = -\frac{i}{\hbar}[H, \rho] + \mathcal{R}\rho \quad (2)$$

In the interaction picture, the atom-light hamiltonian  $H$  and relaxation matrix  $\mathcal{R}\rho$  become

$$\frac{H}{\hbar} = \begin{pmatrix} \Delta_1 & 0 & \Omega_1 \\ 0 & \Delta_2 & \Omega_2 \\ \Omega_1 & \Omega_2 & 0 \end{pmatrix}; \mathcal{R}\rho = \begin{pmatrix} \Gamma_{31}\rho_{33} & -\gamma_c\rho_{12} & -\gamma_{c1}\rho_{13} \\ -\gamma_c\rho_{21} & \Gamma_{32}\rho_{33} & -\gamma_{c2}\rho_{23} \\ -\gamma_{c1}\rho_{31} & -\gamma_{c2}\rho_{32} & -\Gamma\rho_{33} \end{pmatrix} \quad (3)$$

The relaxation matrix includes the spontaneous emission rates  $\Gamma = \Gamma_{31} + \Gamma_{32}$ , optical decoherences  $\gamma_{c1}, \gamma_{c2}$ , and the Raman decoherence  $\gamma_c$  (see Fig. 1(a)). Electric and/or magnetic dipole couplings determine the Rabi frequencies  $\Omega_i$  ( $i = 1, 2$ ). Eq. (2) describes the dynamics of a closed  $\Lambda$ -system where optical detunings  $\Delta_i$  include ac Stark shifts  $\eta_i$  from non-resonant electric-dipole couplings of  $|1\rangle$  and  $|2\rangle$  to other states. For  $\Omega_1, \Omega_2 \lesssim \Gamma_{31}, \Gamma_{32}, \gamma_{c1}, \gamma_{c2}$ , the population in state  $|3\rangle$  is slaved to the population difference  $\Delta n(t) \equiv \rho_{22}(t) - \rho_{11}(t)$  and Raman coherence  $\rho_{12}(t)$ . This allows finding analytical solutions to Eq. (2) by adiabatic elimination of the intermediate state  $|3\rangle$  [20, 21]. The reduced two-level system dynamics are described by a Bloch-vector representation [22, 23].

To remove ac Stark shifts while maintaining a high signal contrast, we apply the Ramsey technique for EIT/Raman fields to this effective two-level system, minimizing systematic frequency shifts over the free-evolution time  $T$ . The Ramsey-like sequence of preparation, free-evolution, and probe, followed by the final destructive detection of the ground state population, is indicated in Fig. 1(c). This eliminates power broadening of the clock transition which is always present for continuous excitation [24]. By solving for the two-level system

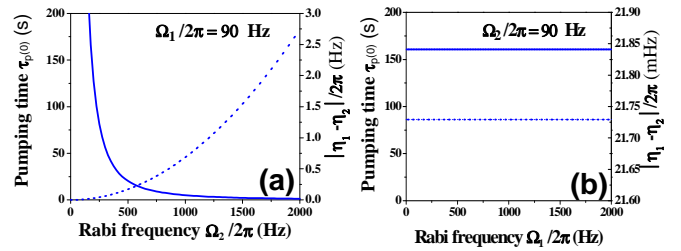


FIG. 2: Differential ac Stark shifts  $\eta_1 - \eta_2$  (dashed curves) on the  $^1S_0 \leftrightarrow ^3P_0$  clock frequency and the optical pumping time  $\tau_p(\Delta_0 = 0)$  (solid curves) using Eq. (6) vs either (a) magnetic Rabi frequency  $\Omega_2$  or (b) electric Rabi frequency  $\Omega_1$ .

using the methods in [23] we can express the populations as

$$\rho_{ii} \equiv \alpha_{ii}(\tau, \tau_m) \left( 1 + \beta_{ii}(\tau, \tau_m) e^{-\gamma_c T} \cos[\delta_r T - \Phi(\tau, \tau_m)] \right) \quad (4)$$

where  $\alpha_{ii}(\tau, \tau_m)$  is the overall envelope function and  $\beta_{ii}(\tau, \tau_m)$  is the amplitude of fringes, both containing exponential decays  $e^{-\tau/\tau_p}$  and  $e^{-\tau_m/\tau_p}$  to their steady states [22].  $\tau_p$  is the characteristic optical pumping time. The atomic phase shift  $\Phi$  produces an approximated clock frequency shift assuming  $\tau, \tau_m \lesssim T$ :

$$\delta\nu = \frac{\Phi(\tau, \tau_m)}{2\pi T(1 + \frac{\tau + \tau_m}{2T})}, \quad (5)$$

which includes all ac Stark contributions accumulated during the pulsed interactions. Hence, a longer free-evolution time  $T$  reduces the light shifts on the clock transition. Furthermore, as will be shown below, a special value  $(\Delta_0)_m$  of the common detuning  $\Delta_0$  can be found to suppress ac Stark effects on the clock frequency. Study of the population dynamics from Eq. (4) leads to an expression for the time  $\tau_p$  that is required to pump atoms into their final steady state, simplified for  $\Delta_0 \simeq \Delta_1 \simeq \Delta_2$ :

$$\tau_p(\Delta_0) \approx \frac{2}{\Gamma} \frac{\Delta_0^2 + \Gamma^2/4}{(\Omega_1^2 + \Omega_2^2)} \left[ 1 - \Upsilon \left( \frac{\Omega_1^2 - \Omega_2^2}{\Omega_1^2 + \Omega_2^2} \right) \right]^{-1}. \quad (6)$$

Here  $\Upsilon = (\Gamma_{31} - \Gamma_{32})/\Gamma$  is the branching ratio difference for the intermediate state which scales the contribution of each Rabi frequency to the pumping rate  $\tau_p^{-1}$ . We emphasize the importance of this time scale as it determines experimental protocols for detecting the EIT or CPT response in either transient or steady states. Previous work on EIT or CPT concentrates mainly on the symmetric case with  $\Upsilon = 0$ . But in the case of alkaline earths where  $\Upsilon \sim \pm 1$ , Eq. (6) shows that the Rabi frequency associated with the weaker transition dictates  $\tau_p$ . For the  $^{88}\text{Sr}$  lattice clock where  $\Gamma_{31} = 2\pi \times 32$  MHz  $\gg \Gamma_{32} = 2\pi \times 620$  Hz (i.e.  $\Upsilon \sim 1$ ), the pumping time at resonance  $\tau_p(0)$  is determined by the magnetic dipole coupling  $\Omega_2$  between  $^3P_0$  and  $^1P_1$ . Figure 2 shows the dependence of  $\tau_p(0)$  on each Rabi frequency while keeping

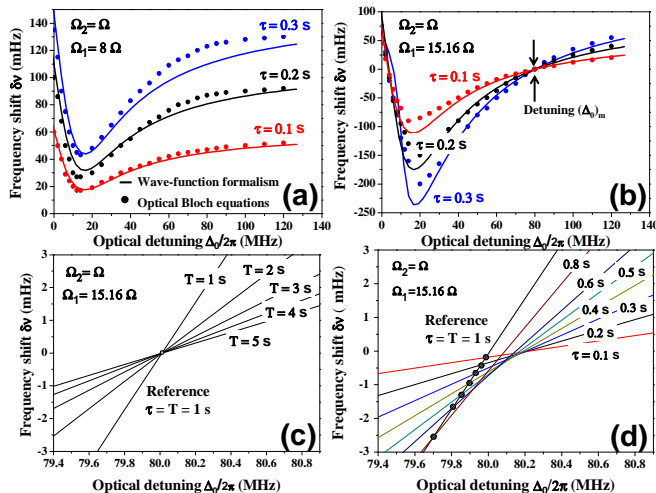


FIG. 3: (Color online) Time diluted frequency shift (Eq. (5) and Eq. (9)) arising from off-resonance ac Stark shift contributions to the  $^1S_0 \leftrightarrow ^3P_0$  transition under different optical detunings  $\Delta_0$ . (a) Three different cases of pulse durations  $\tau = \tau_m$  are shown, under  $T = 1$  s and  $\Omega_1/\Omega_2 = 8$ . Numerical calculations based on Eq. (2) (solid dots) agree with analytical results from the wave-function formalism. The pumping time at resonance is  $\tau_p(0) = 5$  s and the common Rabi frequency is  $\Omega = \sqrt{\Gamma/4\tau_p(0)}$ . (b) Same as (a) except  $\Omega_1/\Omega_2 = 15.16$ , showing Stark shift cancellation near  $(\Delta_0)_m = 80$  MHz. (c) A zoomed-in plot of  $\delta\nu$  versus  $\Delta_0$ , with the slope reduced for a longer  $T$ . The location of the common crossing point is  $(\Delta_0)_m$ . (d)  $\delta\nu$  under different  $\tau$  around  $(\Delta_0)_m$ . The crossings (shown as solid dots) between lines indicate that the same  $\delta\nu$  is obtained for different values of  $\tau$ .

the other one fixed. The dotted lines are the corresponding differential ac Stark shift of the clock frequency in the steady state regime. Note that small ac Stark shifts correspond to long optical pumping times conflicting with realistic clock duty cycles. For instance, the proposal by [10] with ac Stark shift below 21.7 mHz for an accuracy of  $2 \times 10^{-17}$  leads to a signal contrast of a few % only after 160 s. The scheme presented here finds a combination of parameters that maximizes contrast while suppressing ac Stark shifts, exploiting the transient dynamics for short pulses and detuned laser fields. Note that due to the highly asymmetric  $\Upsilon$ , this scheme can uniquely exploit ground-state detection with a high-contrast narrow resonance manifested in the atomic population transfer [25]. In the region of detuning between Raman spectroscopy ( $\Delta_0/\Gamma \gg 1$ ) and EIT/CPT ( $\Delta_0/\Gamma \ll 1$ ), we find contrasts of up to 60%, even though  $\tau \ll \tau_p(\Delta_0) \simeq 100$  s. This same approach could be extended easily to the four level scheme [11], the magnetic induced optical transition [6] (with the magnetic field and the common detuning as operational parameters), or any other clock configurations involving dark states.

The small difference between the field-free clock detuning  $\delta_r$  and the ac Stark shifted detuning  $\Delta_1 - \Delta_2 = (\eta_1 - \eta_2) + \delta_r$  under laser fields leads to a small phase shift of the Ramsey-EIT fringe defined by  $\Phi(\tau, \tau_m)$  in Eq. (5)

[20, 21]. Solving Eq. (2) numerically, we find that a judicious choice of the laser detuning  $(\Delta_0)_m$  cancels the external ac Stark shifts, minimizing the influence to the clock transition when high field strengths are used to rapidly drive EIT resonances. To confirm these results, we also establish an analytical expression for  $\Phi(\tau, \tau_m)$  based on the atomic wave-function formalism [26], using the Hamiltonian of Eq. (3) adding only the term  $-i\Gamma/2$  associated with spontaneous relaxation [27, 28] and neglecting all lattice decoherences. By adiabatic elimination of state  $|3\rangle$ , within an effective two-level system including only the clock states  $|1\rangle$  and  $|2\rangle$ , the amplitudes evolve with a matrix  $M$ , generalized from Ref.[29] by assuming  $\Delta_1 \neq \Delta_2$ :

$$M = \begin{pmatrix} \cos\left(\frac{\omega}{2}t\right) + i\frac{\Delta_{\text{eff}}}{\omega} \sin\left(\frac{\omega}{2}t\right) & 2i\frac{\Omega_{\text{eff}}}{\omega} \sin\left(\frac{\omega}{2}t\right) \\ 2i\frac{\Omega_{\text{eff}}}{\omega} \sin\left(\frac{\omega}{2}t\right) & \cos\left(\frac{\omega}{2}t\right) - i\frac{\Delta_{\text{eff}}}{\omega} \sin\left(\frac{\omega}{2}t\right) \end{pmatrix} \equiv \begin{pmatrix} M_+ & M_{\dagger} \\ M_{\dagger} & M_- \end{pmatrix} \quad (7)$$

where  $\omega = (\Delta_{\text{eff}}^2 + 4\Omega_{\text{eff}}^2)^{1/2}$  and  $\Delta_{\text{eff}}$  ( $\Omega_{\text{eff}}$ ) is the complex detuning (Rabi frequency) in the effective two-level system, extending the definitions of [30]:

$$\Delta_{\text{eff}} = \Omega_1^2 \frac{\Delta_1 + i\Gamma/2}{\Delta_1^2 + \Gamma^2/4} - \Omega_2^2 \frac{\Delta_2 + i\Gamma/2}{\Delta_2^2 + \Gamma^2/4} - (\Delta_1 - \Delta_2) \quad (8)$$

$$\Omega_{\text{eff}} = \Omega_1 \Omega_2 \left( \frac{\Delta_1 + i\Gamma/2}{\Delta_1^2 + \Gamma^2/4} \times \frac{\Delta_2 + i\Gamma/2}{\Delta_2^2 + \Gamma^2/4} \right)^{1/2}$$

The atomic phase depends not only on the wave-function coefficients of the atomic evolution but also on the steady states included in the closed density matrix equations [31]. However, when short pulses  $\tau, \tau_m \ll \tau_p(\Delta_0)$  are applied, stationary solutions can be ignored. For initial conditions  $\rho_{11}(0) = 1, \rho_{22}(0) = 0$ , we find an expression for the atomic phase related to the clock frequency shift:

$$\Phi(\tau, \tau_m) \sim \text{Arg} \left[ \frac{M_-(\tau_m) M_{\dagger}(\tau)}{M_{\dagger}(\tau_m) M_+(\tau)} \right] \quad (9)$$

We are able to find values of  $(\Delta_0)_m$  where the clock shift is suppressed for different practical choices of Rabi frequencies  $\Omega_i$ . Fig. 3(a) plots the clock frequency shift ( $\delta\nu$  as defined in Eq. (5)) versus  $\Delta_0$  under three different cases of  $\tau = \tau_m$ , with  $T = 1$  s and  $\Omega_1/\Omega_2 = 8$ . The dots show numerical results from Eq. (2) and solid curves are analytical results from Eq. (9). Here, we find a non-vanishing  $\delta\nu$  under all conditions. However, as the ratio of  $\Omega_1/\Omega_2$  increases, we do find both approaches give the same value of  $(\Delta_0)_m$  where clock shift is suppressed, as indicated in Fig. 3(b). When different free evolution times ( $T$ ) or pulse durations ( $\tau = \tau_m$ ) are used, the accumulated phase shift changes, leading to variations in the dependence of  $\delta\nu$  on  $\Delta_0$ , as shown in the expanded view of Fig. 3(c) and (d). To determine the optimum value of  $(\Delta_0)_m$  for a practical clock realization at  $\tau = 1$  s, we can use two different techniques. First, as shown in Fig. 3(c), extending  $T$  reduces the sensitivity of  $\delta\nu$  on  $\Delta_0$ . Hence, the curves depicting  $\delta\nu$  versus  $\Delta_0$  for different  $T$  rotate around  $(\Delta_0)_m$ , with no changes in the signal contrast. In

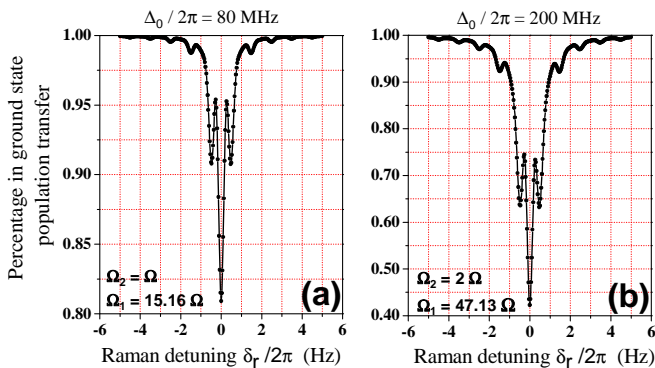


FIG. 4: (Color online) Theoretical EIT/Raman lineshapes using Eq. (4) for the clock transition  $^1S_0 \leftrightarrow ^3P_0$  and a free evolution time  $T = 1$  s. (a) Population transfer of 20% under  $\tau_p(80 \text{ MHz}) = 135$  s and (b) population transfer of nearly 60% under  $\tau_p(200 \text{ MHz}) = 200$  s. The actual pulse durations are  $\tau = \tau_m = 1$  s.

the second approach, as shown in Fig. 3(d), we find the values of  $\Delta_0$  where  $\delta\nu$  for  $\tau = 1$  s is the same as that for some other values of  $\tau$  ( $< 1$  s). These values of  $\Delta_0$  can be plotted as a function of  $\tau$  and extrapolated to  $\tau = 0$  to find  $(\Delta_0)_m$ . However, the signal contrast under smaller  $\tau$  is reduced due to the effect of pulse preparation on population transfer.

From Eq. (4) we find spectral lineshapes and transition probabilities as a function of the experimental parameter  $\delta_r$ , shown in Fig. 4(a). Since  $\tau \ll \tau_p(\Delta_0)$ , the two-photon resonance has a Fourier transform linewidth given by the duration  $\tau$  where power broadening effects

have been eliminated. The spectra also exhibit the typical coherent Ramsey nutations with period  $\sim 1/2T$  and a central fringe free from systematic shifts. We have also determined the sensitivity of  $\delta\nu$  to laser intensities ( $\Omega_i$ ) and detunings, demonstrating that the uncertainty of the optical clock frequency  $< 5$  mHz ( $\sim 10^{-17}$ ) is achievable by controlling  $\Delta_0$  at the 100 kHz level around  $(\Delta_0)_m$ . Meanwhile,  $\Omega_i$  fluctuations should be controlled  $< 0.5\%$ . We note that for a given set of  $\tau$  and  $\Omega_i$ , different values of  $(\Delta_0)_m$  can be found. For example,  $(\Delta_0)_m = 200$  MHz is another optimum value for larger  $\Omega_i$  (Fig. 4 (b)). In this case, the signal contrast is further improved with a population transfer of up to 60%, leading to enhanced clock stability but also slightly larger uncertainty.

In summary, our method achieves the  $10^{-17}$  accuracy expected for a “light-insensitive” lattice clock with EIT/Raman pulses to dilute fluctuations of the frequency shift over the free evolution time  $T$ . We show that a contrast between 20% to 60% (Fig. 4) could be achieved, also including realistic lattice decoherence times [4]. Extensions are possible to the proposal of [11] by replacing the  $^1P_1$  state with  $^3P_1$ , to magnetic field induced optical transitions [6], for other species like  $^{52}\text{Cr}$  [32], and for nuclear clock transitions [33].

We thank J. Dalibard, T. Ido, T. Zelevinsky, and C. Oates for discussions. This work is supported by ONR, NIST, and NSF. T. Zanon thanks Observatoire de Paris and Délégation Générale de l’Armement for support.

\*Present address: Laser Cooling and Trapping Group, NIST Gaithersburg, MD-20899, USA; permanent address: Dipartimento di Fisica, Università di Pisa, Italy.

- 
- [1] P.O. Schmidt *et al.*, *Science* **309**, 749 (2005); H.S. Margolis *et al.*, *Science* **306**, 1355 (2004); T. Schneider, E. Peik, and C. Tamm, *Phys. Rev. Lett.* **94**, 230801 (2005); P. Dube *et al.*, *Phys. Rev. Lett.* **95**, 033001 (2005).
- [2] U. Sterr *et al.*, *C. R. Physique* **5**, 845 (2004); F. Ruschewitz *et al.*, *Phys. Rev. Lett.* **80**, 3173 (1998); T. Ido *et al.*, *Phys. Rev. Lett.* **94**, 153001 (2005).
- [3] M. Takamoto *et al.*, *Nature* **435**, 321 (2005).
- [4] A. Ludlow *et al.*, *Phys. Rev. Lett.* **96**, 033003 (2006).
- [5] R. Le Targat *et al.*, *Phys. Rev. Lett.* **97**, 130801 (2006).
- [6] Z.W. Barber *et al.*, *Phys. Rev. Lett.* **96**, 083002 (2006).
- [7] M.M. Boyd *et al.*, arXiv:physics/0610096 (2006).
- [8] S. Bize *et al.*, *J. Phys. B: At. Mol. Opt. Phys.* **38**, S449 (2005); T. P. Heavner *et al.*, *Metrologia* **42**, 411 (2005).
- [9] H. Katori *et al.*, *Phys. Rev. Lett.* **91**, 173005 (2003).
- [10] R. Santra *et al.*, *Phys. Rev. Lett.* **94**, 173002 (2005).
- [11] T. Hong *et al.*, *Phys. Rev. Lett.* **94**, 050801 (2005).
- [12] H. Häffner *et al.*, *Phys. Rev. Lett.* **90**, 143602 (2003).
- [13] J.A. Sherman *et al.*, *Phys. Rev. Lett.* **94**, 243001 (2005).
- [14] A. Brusch *et al.*, *Phys. Rev. Lett.* **96**, 103003 (2006).
- [15] M. Fleischhauer, A. Imamoglu, and J.P. Marangos, *Rev. Mod. Phys.* **77**, 633 (2005).
- [16] P. Knight, *Nature* **297**, 16 (1982).
- [17] A. Morinaga, T. Tako, and N. Ito, *Phys. Rev. A* **48**, 1364 (1993). K. V. R. M. Murali *et al.*, *Phys. Rev. Lett.* **93**, 033601 (2004).
- [18] E. Arimondo, *Progress in Optics* **35**, 257 (1996).
- [19] R. Santra, K.V. Christ, and C.H. Greene, *Phys. Rev. A* **69**, 042510 (2004).
- [20] P.R. Hemmer *et al.*, *J. Opt. Soc. Am. B* **6**, 1519 (1989).
- [21] M.S. Shahriar *et al.*, *Phys. Rev. A* **55**, 2272 (1997).
- [22] E.T. Jaynes, *Phys. Rev.* **98**, 1099 (1955).
- [23] R.L. Schoemaker, in “**Laser and coherence spectroscopy**”, Ed. J.I. Steinfeld, New York, Plenum Press, 197 (1978).
- [24] T. Zanon *et al.*, *Phys. Rev. Lett.* **94**, 193002 (2005).
- [25] I.V. Jyotsna and G.S. Agarwal, *Phys. Rev. A* **52**, 3147 (1995).
- [26] J. Dalibard, Y. Castin, and K. Mølmer, *Phys. Rev. Lett.* **68**, 580 (1992).
- [27] P.M. Radmore and P.L. Knight, *J. Phys. B: At. Mol. Phys.* **15**, 561 (1982).
- [28] Y. Stalgies *et al.*, *J. Opt. Soc. Am. B* **15**, 2505 (1998).
- [29] T. Zanon *et al.*, *IEEE Trans. Instrum. Meas.* **54**, 776 (2005).
- [30] K. Moler, D.S. Weiss, M. Kasevich, S. Chu, *Phys. Rev. A* **45**, 342 (1992).
- [31] G. Orriols, *Il Nuovo Cimento. B* **53**, 1 (1979).

- [32] A.S. Bell *et al.*, EuroPhys. Lett. **45**, 156 (1999).
- [33] E. Peik and C. Tamm, EuroPhys. Lett. **61**, 181 (2003).